Available online at www.sciencedirect.com

ScienceDirect

Ciência & Tecnologia dos Materiais 28 (2016) 81–87

Ciência & Tecnologia dos MATERIAIS

http://ees.elsevier.com/ctmat

Special Issue on New Challenges in Energy Materials

Water management in PEMFC: 1-D model simulations

D.S. Falcão*, C. Pinho, A.M.F.R. Pinto*

CEFT-DEQ, Faculdade de Engenharia da Universidade do Porto, Rua Dr. Roberto Frias, 4200-465 Porto – Portugal

Abstract

The water management is a critical problem to overcome in the PEM fuel cell technology. Models play an important role in fuel cell development since they enable the understanding of the influence of different parameters on the cell performance allowing a systematic simulation, design and optimization of fuel cells systems. In this work, a model previously developed and validated, is used to predict the water transport through the cell. The influence of membrane thickness and transport properties, reactants pressure and relative humidity and operation temperature, on the water content through the membrane and on the cell performance was studied. The model predicts the membrane water content and water concentration profiles across the membrane electrode assembly (MEA). This work represents a useful tool to set-up suitable operating conditions leading to an optimised water management producing a better performance for PEM fuel cells.

Keywords: PEM Fuel cells, electrochemistry, mathematical model, water management.

1. Introduction

Fuel cells are an innovative alternative to current power sources with potential to achieve higher efficiencies with renewable fuels with minimal environmental impact. In particular, the proton-exchange membrane (PEM) fuel cells are today in the focus of interest as one of the most promising developments in power generation with a wide range of applications in transportation and in portable electronics. Although prototypes of fuel cell vehicles and residential fuel cell systems have already been introduced, their cost must be reduced and their efficiencies enhanced.

Several coupled fluid flow, heat and mass transport processes occur in a fuel cell together with the electrochemical reactions. Generally, PEMFC operate bellow 80ºC. Anodic oxidation of hydrogen produces protons that are transported through the membrane to the cathode where the reduction of oxygen generates water. One of the most important operational issues of PEMFC is the water management in the cell [1-3].

The water content of the membrane is determined by the balance between water production and three water transport processes: electro-osmotic drag of water (EOD), associated with proton migration through the membrane; back diffusion from the cathode to the anode and diffusion of water to/from the oxidant/fuel gas streams. Understanding the water transport in the PEM is a key issue. To achieve optimal fuel cell performance, it is critical to have an adequate water balance to ensure that the membrane remains hydrated for sufficient proton conductivity, while cathode flooding and anode dehydration are avoided [4-7].

To improve the system performance, design optimization and analysis of fuel cell systems are important. Mathematical modelling and simulation are needed as tools for design optimization of fuel cells, stacks and fuel cells power systems [8,9].

* Corresponding authors.
E-mail addresses: *dfalcao@fe.up.pt* (D.S. Falcão), *apinto@fe.up.pt* (A.M.F.R. Pinto),

http://dx.doi.org/10.1016/j.ctmat.2016.12.001

Different models were developed in the last decade to describe several water transport mechanisms through the membrane such as Springer et al. [10] using a diffusion model, Bernardi and Verbrugge [11] considering a hydraulic permeation model and Kulikovsky [12] developing a semi analytical model 1D+1D taking into account oxygen and water transport across the cell and deriving an expression for the limiting current density. A novel approach coupling neutron imaging and numerical modelling for the analysis of the impact of water on fuel cell performance was used to analyze a 1D cell and the effective diffusion coefficient is calculated from the results of the combination of modelling and experimental data [13]. Numerical simulations using the Volume of Fluid (VOF) method to simulate the droplets inside the channels have been crucial to complement experimental results by giving quantitative information about the two-phase flow in PEM fuel cells and its effects [14, 15].

In order to make proper simulations, previously or alternatively to the execution of experimental tests, it is very useful the help provided by a reduced model, easy to implement and with low running times. However, to obtain trustworthy results all the model parameters should be carefully selected.

In a previous work, Falcão et al [16] developed a semi-analytical one-dimensional model considering the effects of coupled heat and mass transfer, along with the electrochemical reactions occurring in PEMFC. The model can be used to predict the hydrogen, oxygen and water concentration profiles in the anode, cathode and membrane, as well as the temperature profile across the cell. The model was validated with published experimental data in work [16] and with experimental data from the authors in reference [17]. This model was also compared with a 3D model [18]. The results showed that the 1D model can be used to predict optimal operating conditions in PEMFCs and the general trends of the impact of several important physical parameters on fuel cell performance. The use of the 3D numerical simulations is indicated if more detailed predictions are needed.

The developed model is used in the present work to study the water management in the PEMFC. In particular, predictions of the influence of the membrane thickness and transport properties, reactants pressure and relative humidity and operation temperature, on the water content are presented.

2. Model simulations

All the model equations and the parameter values used to obtain the results presented in the next section can be found in a previous work [16], with an updating in the expressions used to predict the anode and cathode overpotentials:

$$\eta_a = \ln\left(\frac{I_{cell}(C_{H_2}^{ref})^{\gamma^a}}{i_0^{ref}(C_{H_2}^{ACL})^{\gamma^a}}\right)\frac{RT}{\alpha_a F} \quad (1)$$

$$\eta_c = \ln\left(\frac{I_{cell}(C_{O_2}^{ref})^{\gamma^c}}{i_0^{ref}(C_{O_2}^{CCL})^{\gamma^c}}\right)\frac{RT}{\alpha_c F} \quad (2)$$

All parameters are carefully chosen from recent literature, namely reference exchange current density and transfer coefficients. Exchange current densities and transfer coefficients are selected based in two specific references [19, 20] concerning the study of the anode and cathode kinetics. Parameters used in equations (1) and (2) are presented in Table 1.

The numerical tools used to implement the model were Matlab and Excel. Due to its importance in PEMFC development, particular attention is devoted, in the present work, to the water management in the cell.

The obtained predictions of the membrane water content and polarization curves after implementation of the model are presented. The conditions used to generate the simulations are summarized in Table 2.

3. Results and discussion

The analysis of the influence of various parameters, such as membrane thickness, reactants pressure and humidity and operating temperature is done in the following sections.

3.1. Influence of membrane thickness

Simulations were done, with four different membrane thicknesses, in order to study the influence of the membrane thickness. The polarization curves obtained are shown in Figure 1. As can be seen from Figure 1, best performances are obtained for Nafion 112 and Gore Select, the thinner membranes. Nafion 117 and Nafion 115 lead to lower performances, for these operating conditions.

Table 1. Kinetic parameters values used in simulations.

Parameter	Value	Reference
E_0 [V]	$1.23 - 0.9 \times 10^{-3}(T - 298) + \frac{2.303RT}{4F} log\left[\left(\frac{P_{H_2}}{P_{H_2}^{ref}}\right)^2 \left(\frac{P_{O_2}}{P_{O_2}^{ref}}\right)\right]$	[19]
i_{0,H_2}^{ref} [A/cm^2]	$i_0^{ref}(T) = i_0^{ref}(T_r)\left(\frac{P_{H_2}}{P_{H_2}^{ref}}\right)^{kro} exp\left[\frac{\Delta E_a}{R}\left(\frac{1}{T_{ref}}\right) - \left(\frac{1}{T}\right)\right]$	Adapted from [20]
i_{0,O_2}^{ref} [A/cm^2]	$i_0^{ref}(T) = i_0^{ref}(T_r)\left(\frac{P_{O_2}}{P_{O_2}^{ref}}\right)^{0.79}\left(\frac{P_{H_2}}{P_{H_2}^{ref}}\right)^{n\alpha_c/2} exp\left[\frac{-\Delta E_c^{0.9V}}{R}\left(\frac{1}{T_{ref}}\right) - \left(\frac{1}{T}\right)\right]$	[19]
$i_{0,H_2}^{ref}(T_r)$ [A/cm^2]	0.267	[20]
$i_{0,O_2}^{ref}(T_r)$ [A/cm^2]	$10 L_{ca} A_{Pt} 1.7 \times 10^{-8}$	[19]
L_{ca}[mg$_{Pt}$/cm^2]	0.5	Assumed
A_{Pt}[m$^2_{Pt}$/g$_{Pt}$]	60	[21]
ΔE_a [A/cm^2]	10 kJ/mol	[22]
ΔE_c [A/cm^2]	67 kJ/mol	[19]
kro	1.0	[21]
α_a	0.5	[20]
α_c	-0.5 I_{cell}+1	Adapted from [19]
γ_a	0.5	[23]
γ_c	1.0	[23]

Thicker membranes provide lower proton conductivities due to lower water retention. Based on this idea, it is useful to calculate the water membrane content (λ) for each membrane used. The simulation results for the membrane water contents are presented in Figure 2.

As can be seen from Figure 2, the membrane water content values are, as expected, lower for thicker membranes; these results are in agreement with the curves from Figure 1. The water content values decrease at the anode side and increase at the cathode side for increasing current densities.

Table 2. Set of conditions used in this work.

Cell Temperature [K]	333
Anode Flow Temperature [K]	333
Anode Relative Humidity [%]	100
Cathode Flow Temperature [K]	333
Cathode Relative Humidity [%]	100
Anode Pressure [atm]	1
Cathode Pressure [atm]	1
Membrane active area [cm^2]	25
Anode and Cathode Diffusion Layer Thickness [cm]	0.02
Anode and Cathode Catalytic Layer Thickness [cm]	0.0012
Membrane Thickness [cm]	0.0127

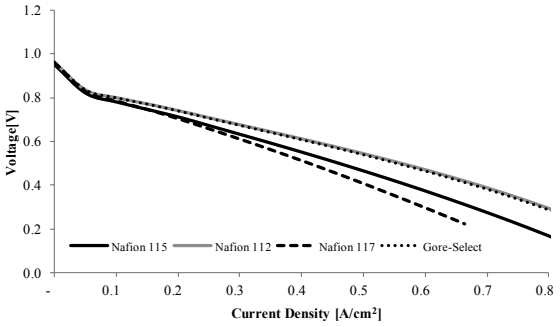

Fig. 1. Voltage vs. current density for different membrane thicknesses: Nafion 112 (0.0051 cm), Nafion 115 (0.0127 cm), Nafion 117 (0.0178 cm) and Gore-Select (0.003 cm) for a flow H_2/air with ζ_a=1 at 1 A/cm^2 and ζ_c=2 at 1 A/cm^2.

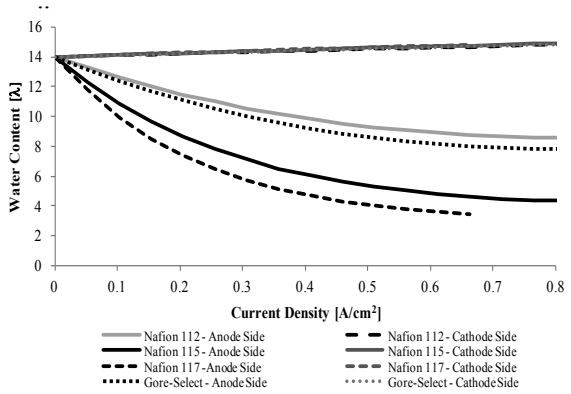

Fig. 2. Membrane water content vs. current density for different membrane thicknesses: Nafion 112 (0.0051 cm), Nafion 115 (0.0127 cm), Nafion 117 (0.0178 cm) and Gore-Select (0.003 cm) for a flow H_2/air with ζ_a=1 at 1 A/cm^2 and ζ_c=2 at 1 A/cm^2.

This occurs due to water production at the cathode side and electro-osmotic drag from the anode to the cathode. In thinner membranes, both water flux and fuel cell performance increase according to a decrease in the mass transfer resistance. Relatively to the two thinner membranes, although Gore-Select is thinner than Nafion 112, the water diffusivity in Gore-Select membrane is half the value of Nafion 112. However, the difference in fuel cell performances, for the operating conditions studied, is not significant. So, both thinner membranes could be used with great advantages in fuel cell performance.

3.2. Influence of reactants pressure

The influence of the reactants pressure was studied for three different inlet pressures. Polarization curves are presented in Figures 3 and 4.

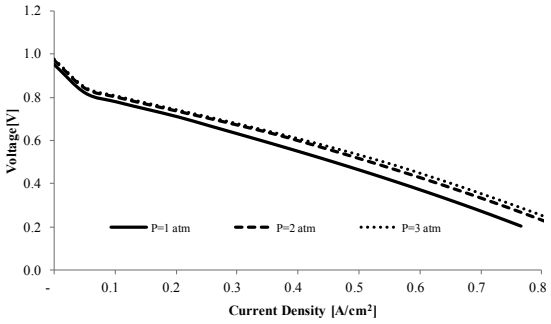

Fig. 3. Voltage vs. current density for different gas inlet pressures for a flow H_2/air with ζ_a=1 at 1 A/cm^2 and ζ_c=2 at 1 A/cm^2.

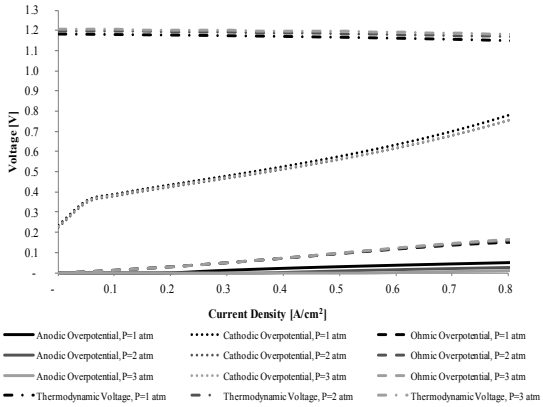

Fig. 4. Anodic, cathodic and ohmic losses and open circuit voltage vs. current density for different gas inlet pressures for a flow H_2/air with ζ_a=1 at 1 A/cm^2 and ζ_c=2 at 1 A/cm^2.

As can be seen in Figure 3, better results are obtained for higher pressures. Pressurized anode and cathode improve oxidation/reduction reactions by an increase in the reactants partial pressure.

Figure 4 shows that, effectively, for higher pressures, the anodic and cathodic losses are slightly lower. Ohmic losses are practically the same for all pressures, so, the increase of reactants pressure has no significant effect in the water management. Relatively to the open circuit voltage, higher values correspond to higher pressures of reactants, which confirm the improvement in fuel cell performance under these conditions.

3.3. Influence of operation temperature

The influence of operation temperature was studied for three different values for fully humidified conditions both at anode and cathode sides. The polarization curves are presented in Figure 5, the membrane water content results are presented in Figure 6 and values for the water diffusivity in the

membrane are presented in Figure 7. Figure 5 shows that better fuel cell performances are obtained for higher operation temperatures.

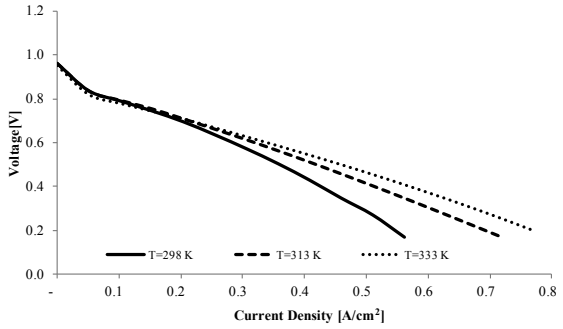

Fig. 5. Voltage vs. current density for different operation temperatures for a flow H_2/air with ζ_a=1 at 1 A/cm^2 and ζ_c=2 at 1 A/cm^2.

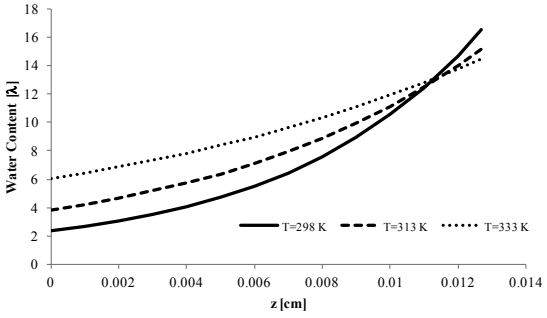

Fig. 6. Membrane water content across the membrane for different operation temperatures for a flow H_2/air with ζ_a=1 at 1 A/cm^2 and ζ_c=2 at 1 A/cm^2 (current density of 0.4 A/cm^2).

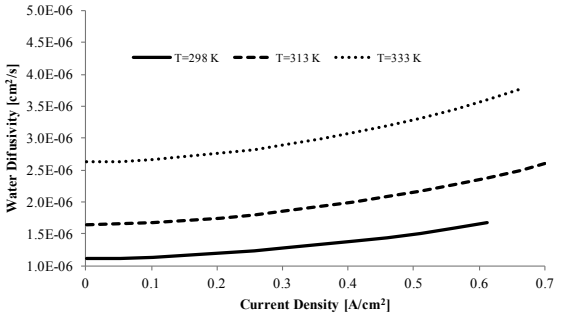

Fig. 7. Water diffusivity vs. current density for different operation temperatures for a flow H_2/air with ζ_a=1 at 1 A/cm^2 and ζ_c=2 at 1 A/cm^2.

The curves in Figure 6 show that, for a current density of 0.4 A/cm^2, the membrane water content values are higher for higher operation temperatures across almost all the membrane thickness except in the last few millimetres, being the average water content higher for the higher operating temperature. The water content increases from the anode to the cathode because, as already referred, at the cathode side water is produced. In the model, calculations related to membrane resistance use an average value of membrane water content, thus lower membrane resistances are obtained for higher values of the average water contents. Therefore, under these operating conditions, fuel cell performance is strongly enhanced by higher operation temperatures. The curves in Figure 7 further confirm these results since as can be seen the membrane water diffusivity increases significantly with the current density and with the temperature. Depending on the water content, the water diffusivity is strongly enhanced by higher temperatures, which in turns promotes higher membrane water contents. Along with the positive effect on the water diffusivity through the membrane, there is also the positive effect of increasing temperature on the reaction rates.

3.4. Influence of relative humidity

The influence of gases relative humidity (RH) was studied for three different conditions: both gases fully humidified and one fully humidified and the other with 50 % RH. Polarization curves, membrane water content prediction and net water transport coefficient results are presented, for the different operating conditions, in Figures 8, 9 and 10, respectively.

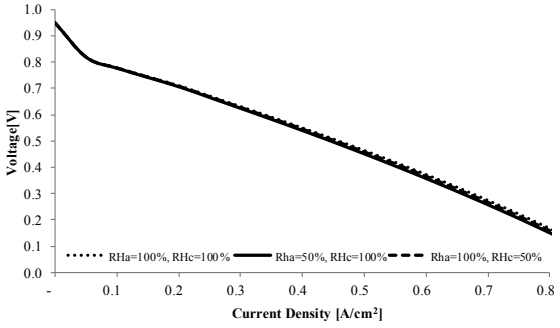

Fig. 8. Voltage vs. current density for different gases relative humidity for a flow H_2/air with ζ_a=1 at 1 A/cm^2 and ζ_c=2 at 1 A/cm^2.

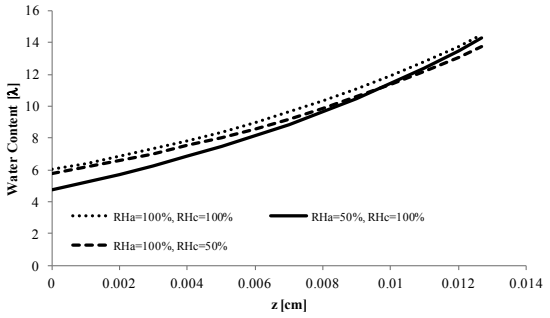

Fig. 9. Membrane water content vs. membrane thickness for different gases relative humidity for a flow H_2/air with ζ_a=1 at 1 A/cm^2 and ζ_c=2 at 1 A/cm^2 (current density of 0.4 A/cm^2).

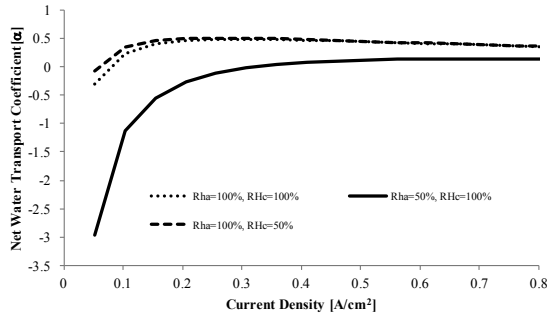

Fig. 10. Net water transport coefficient vs. membrane thickness for different gases relative humidity for a flow H_2/air with ζ_a=1 at 1 A/cm^2 and ζ_c=2 at 1 A/cm^2.

Figure 8 shows that the better fuel cell performance is achieved when both gases are fully humidified. It should be also noted that fuel cell performance is lower when the anode humidification is lower.

In Figure 9, higher values of the water content are obtained when both gases are fully humidified corresponding to higher fuel cell performances. When the anode side is partially humidified, the water content is lower at the anode side but increases at the cathode side due to water production. When the cathode side is partially humidified, the water content also increases across the membrane but values for the anode side are higher than those obtained for the previous condition.

In order to better understand the water transport mechanisms occurring in this situation, the values of the net water transport coefficient versus current density are represented in Figure 10. It should be noted that positive values of α correspond to a net water flow from anode to cathode while negative values indicate that the net flow occurs forward the anode. The plots show that, when the anode side is partially humidified, water is transferred from the cathode to the anode by water back diffusion. For the other two conditions, the α values are low but positive, which indicates that water is transferred by electro-osmotic drag but the flux is low. As already referred, due to water production at the cathode, the introduction of water in cathode side is not as necessary as it is at the anode side.

4. Conclusions

In the present study, a previous developed model is used to predict the influence of the membrane thickness, of the operation temperature, of the reactants pressure and relative humidity on the water content through the membrane and on the cell performance.

For all cases studied, a better performance fuel cell result corresponds to higher water contents in the membrane.

Cell performance was improved by using thinner membranes because the water flux through membrane increases (lower resistance to mass transfer).

Higher inlet gases pressure improves fuel cell performance since anode and cathode losses decrease and the open circuit voltage increase.

The operation temperature has a large influence in fuel cell performance; better results are obtained for higher operation temperatures because the water diffusivity strongly increases with operation temperature.

Relatively to the gases relative humidity, the fuel cell performance is improved when both gases are fully humidified. Anode humidification is more necessary than cathode humidification, for these operating conditions.

This easy to implement model is useful to achieve adequate operating conditions to different applications in real time. Much time and effort could be saved if a simple but robust model is used to make simulations previously to the execution of experimental tests.

Acknowledgements

D.S. Falcão acknowledges the post-doctoral fellowship (SFRH/BDP/76063/2011) supported by the Portuguese "Fundação para a Ciência e Tecnologia" (FCT), POPH/QREN and European Social Fund (ESF). POCI (FEDER) also supported this work via CEFT.

List of symbols

A_{Pt}	Available Pt surface area [m^2_{Pt}/g_{Pt}]
F	Faraday's constant [C/mol]
E_0	Open circuit voltage (V)
I_{cell}	Current density [A/cm^2]
i_0	Exchange current density [A/cm^2]
L_{ca}	Cathode Pt loading [mg_{Pt}/cm^2]
kro	Kinetic reaction order
R	Universal gas constant [J/mol.K]
T	Temperature [K]
Greek letters	
γ^a	Anode concentration dependence
γ^c	Cathode concentration dependence
η	Overpotential [V]
α_a	Anode transfer coefficient
α_c	Cathode transfer coefficient
ΔE	Activation Energy[kJ/mol]
Subscripts	
H_2	Hydrogen
O_2	Oxygen
Superscripts	
a	anode
c	cathode
ACL	Anode catalyst layer
CCL	Cathode catalyst layer
Ref	Reference value

References

[1] M. Eikerling, Y.I. Kharkats, A.A. Kornyshev, Y.M. Volfkovich, J. Electrochem. Soc. 145 (1998) 2684.
[2] M. Eikerling, A.A. Kornyshev, A.R. Kucernak, Physics Today, 59 (2006) 38.
[3] Y. Wang, K.S. Chen, J. Mishler, S.C. Cho, X.C. Adroher, Appl. Energy 88, (2011) 981.
[4] J.J. Baschuk and X. Li, J. Power Sources 86 (2000) 181.
[5] A. BiyIkoglu, Int. J. Hydrogen Energy 30 (2005) 1181.
[6] H. Chang, J.R. Kim, J.H. Cho, H.K. Kim, K.H. Choi, Solid State Ionics 148 (2002) 601.
[7] R. Anderson, L. Zhang, Y. Ding, M. Blanco, X. Bi, D.P. Wilkinson, J. Power Sources 195 (2010) 4531.
[8] M.M. Nasef and A.A. Aly, Desalination 287 (2012) 238.
[9] V. Liso, S. Simon Araya, A.C. Olesen, M.P. Nielsen, S.K. Kær, Int. J. Hydrogen Energy 41 (2016) 3079.
[10] T.E. Springer, T.A. Zawodzinski, S. Gottesfeld, J. Electrochem. Soc. 138, (1991) 2334.
[11] D.M. Bernardi, M.W. Verbrugge, J. Electrochem. Soc. 139 (1992) 2477.
[12] A.A. Kulikovsky, Electrochem. Commun. 6 (2004) 969.
[13] A. Iranzo, P. Boillat, P. Oberholzer, J. Guerra, Energy 68 (2014) .
[14] R.B. Ferreira, D.S. Falcão, V.B. Oliveira, A.M.F.R. Pinto, J. Power Sources 277 (2015).
[15] R.B. Ferreira, D.S. Falcão, V.B. Oliveira, A.M.F.R. Pinto, Energy 82 (2015) 619.
[16] D.S. Falcão, V.B. Oliveira, C.M. Rangel, C. Pinho, A.M.F.R. Pinto, Chem. Eng. Sci. 64 (2009) 2216.
[17] D.S. Falcão, C.M. Rangel, C. Pinho, A.M.F.R. Pinto, Energ Fuels 23 (2008) 397.
[18] D.S. Falcão, P.J. Gomes, V.B. Oliveira, C. Pinho, A.M.F.R. Pinto, Int. J. Hydrogen Energy 36, (2011) 12486.
[19] K.C.G. Neyerlin, W.; Jorne, J.; Gasteiger, H.A., J. Electrochem. Soc. 153 (2006) A1955.
[20] K.C.G. Neyerlin, W.; Jorne, J.; Gasteiger, H.A., J. Electrochem. Soc.154 (2007) B631.
[21] C.S. Spiegel, PEM Fuel Cell Modeling and Simulation Using MATLAB. 2008: Elsevier.
[22] J. Jiang and A. Kucernak, J. Electroanal. Chem. 567 (2004) 123.
[23] C.H. Min, Y.L. He, X.L. Liu, B.H. Yin, W. Jiang, W.Q. Tao, J. Power Sources 160 (2006) 374.